

# Finding Critical Nucleus in Solid-State Transformations

CHEN SHEN, JU LI, and YUNZHI WANG

Based on the phase-field total free energy functional and free-end nudged elastic band (NEB) algorithm, a new methodology is developed for finding the saddle-point nucleus in solid-state transformations. Using cubic  $\rightarrow$  tetragonal transformations in both two and three dimensions as examples, we show that the activation energy and critical nucleus configuration along the minimum energy path (MEP) can be determined accurately and efficiently using this new approach. When the elastic energy contribution is dominant, the nucleation process is found to be collective with the critical nucleus consisting of two twin-related variants. When the elastic energy contribution is relatively weak, the critical nucleus consists of a single variant, and the polytwinned structure develops during growth through a stress-induced autocatalytic process. A nontrivial two-variant critical nucleus configuration is observed at an intermediate level of the elastic energy contribution. This general method is applicable to any thermally activated process in anisotropic media, including nucleation of stacking faults and dislocation loops, voids and microcracks, and ferroelectric and ferromagnetic domains. It is able to treat nucleation events involving simultaneously displacive and diffusional components, and heterogeneous nucleation near pre-existing lattice defects.

DOI: 10.1007/s11661-007-9302-7

© The Minerals, Metals & Materials Society and ASM International 2007

## I. INTRODUCTION

NUCLEATION during solid-state reactions (*e.g.*, phase transformations, plastic deformation, fracture, *etc.*) is by far one of the most difficult problems to deal with in materials research, irrespective of the method of study, *i.e.*, experimental, analytical, or numerical. This is because the actual nucleation process is a rare event and the saddle-point configuration only exists transiently. The existing nucleation models, both classical and nonclassical, assume only a limited number of degrees of freedom for the nucleus and do not provide a complete sampling over all possible structural and compositional configurations.

The nonclassical nucleation theory of Cahn and Hilliard<sup>[1]</sup> based on the gradient thermodynamics of nonuniform systems<sup>[2]</sup> provides a general framework for treating nucleation. Rather than assuming a particular geometry for a critical nucleus that has bulk properties of the equilibrium product phase and is separated from the parent phase by a sharp interface, it characterizes the nucleus as composition nonuniformity by using a concentration field, and the critical nucleus is determined by the saddle point of the total free energy functional. It was demonstrated<sup>[1]</sup> that in the limit of

small supersaturation, the nonclassical theory reproduces all features predicted by the classical nucleation theory. The theory can be extended to nucleation of structural nonuniformities as well.<sup>[3–6]</sup>

Since the microstructural features developed during solid-state reactions are often influenced by elastic strain fields that are in general functions of size, shape, spatial orientation, and mutual arrangement of the existing compositional and structural nonuniformities,<sup>[7]</sup> a rigorous treatment of nucleation in solids requires a self-consistent description of the interactions between the nucleus and the pre-existing microstructure without any *a priori* assumptions. Based on gradient thermodynamics<sup>[2]</sup> and microelasticity theory,<sup>[7]</sup> the phase field approach is a superset of the Cahn–Hilliard description of chemical inhomogeneities and the Peierls (cohesive zone) description of displacive inhomogeneities<sup>[8]</sup> and therefore can treat nucleation of various types of extended defects produced by both displacive and diffusional processes (for recent reviews, see References 9–13). However, the difficulty in this approach is to locate the exact saddle point in a configuration space of very high dimensions. Analytical approaches, though undoubtedly useful in theoretical analysis, are limited to a few simple systems. The numerical approaches<sup>[14,15]</sup> are generally expensive and less stable because the saddle point is an unstable stationary point.

In this article, we develop an effective approach for determining accurately the critical nucleus configuration and the minimum energy path (MEP) of a thermally activated process by combining phase-field energetics with the nudged elastic band (NEB) method.<sup>[16]</sup> The approach takes advantage of the generality of the phase-field total free energy functional (in particular, its ability to describe arbitrary nonuniformities in the presence of long-range interactions), the ability of the free-end NEB

---

CHEN SHEN, Research Associate, and JU LI and YUNZHI WANG, Professors, are with the Department of Materials Science and Engineering, The Ohio State University, Columbus, OH 43210, USA. Contact e-mail: wang.363@osu.edu

This article is based on a presentation given in the symposium entitled “Solid-State Nucleation and Critical Nuclei during First Order Diffusional Phase Transformations,” which occurred October 15–19, 2006 during the MS&T meeting in Cincinnati, Ohio under the auspices of the TMS/ASM Phase Transformations Committee.

Article published online September 28, 2007

(FE-NEB) method to search for the optimal reaction coordinate without any *a priori* assumptions, and the Langevin force approach that provides the initial free-end configuration for the FE-NEB method. The NEB calculations require only the total free energy and its first-order derivatives (variations), which are straightforward and inexpensive to obtain from a phase-field model. This approach has been implemented previously for dislocation-level plasticity studies.<sup>[17]</sup> In Section II, we outline a general procedure of integrated phase-field total free energy functional + FE-NEB + Langevin dynamics (for end configuration generation) approach for studying various activation processes in microstructure evolution during solid-state reactions. In Section III, the new approach is demonstrated by its application to a cubic  $\rightarrow$  tetragonal transformation. Discussion and summary are presented, respectively, in Sections IV and V.

## II. METHOD

The phase-field total free energy functional defines a hypersurface in an  $M \times P$ -dimensional phase-field configuration space, where  $M$  is the number of real-space grid points and  $P$  the number of phase fields (order-parameter fields that could be chemical or structural). On the surface located are microstructural configurations that correspond to stable and metastable states and saddle points, connected by MEPs. According to transition state theory,<sup>[18]</sup> the highest saddle point along the MEP defines the critical nucleus configuration and the activation energy that determines the rate of a reaction.<sup>[18]</sup> The saddle points are the solutions of vanishing variation of the total free energy functional subject to external constraints. Because they are unstable stationary points, the conventional phase-field dynamic equations governed by total free energy minimization are incapable of obtaining the exact solution, even with the use of Langevin force terms. Finding saddle points, however, is a well-studied subject in theoretical chemistry and condensed matter physics. The NEB method<sup>[19–21]</sup> has been shown as a reliable approach to find the MEP that passes the saddle point. With the climb-image NEB (CI-NEB) technique,<sup>[16,22]</sup> the exact saddle configuration and energy can be identified.

Originally, finding the saddle point in NEB calculations must start with two fixed end configurations such as a completely transformed product phase and a completely untransformed parent phase matrix. This choice, however, often results in a poor resolution of the activation energy barrier, because the barrier is usually very small as compared to the change in the total free energy as the entire matrix is transformed. The FE-NEB method developed recently<sup>[23,24]</sup> can resolve this problem by taking a partially transformed matrix as one end configuration. This FE configuration can be chosen not far beyond the saddle point. Since it is required to be only roughly along the MEP, such a configuration is not difficult to produce in the conventional phase-field method using Langevin fluctuations.

Consider a generic phase field model with a set of  $P$ -phase fields,  $\phi \equiv \{\phi_\alpha(\mathbf{x}) : \alpha = 1, \dots, P\}$ , that describe

a given microstructure. The term  $\mathbf{x}$  is the spatial coordinate. The total free energy of the system is formulated as a functional of the phase fields

$$G = G[\{\phi_\alpha\}] = \int [f(\{\phi_\alpha(\mathbf{x})\}) + \sum_{\alpha,\beta} \kappa_{\alpha\beta} \nabla \phi_\alpha(\mathbf{x}) \nabla \phi_\beta(\mathbf{x})] d\mathbf{x} + \int \sum_{\alpha,\beta} B_{\alpha\beta}(\mathbf{k}) \tilde{\phi}_\alpha(\mathbf{k}) \tilde{\phi}_\beta^*(\mathbf{k}) \frac{d\mathbf{k}}{(2\pi)^3} - \int \sigma^{\text{ext}}(\mathbf{x}) \varepsilon(\{\phi_\alpha(\mathbf{x})\}) d\mathbf{x} \quad [1]$$

which contains contributions from local energy density  $f$ , spatial gradient of the fields (in the first integral), long-range interactions (*e.g.*, elastic, electrostatic or magnetostatic interactions) that are formulated in the reciprocal ( $\mathbf{k}$ ) space, and interaction with external fields,  $\sigma^{\text{ext}}$ . The gradient coefficient  $\kappa_{\alpha\beta}$  can be formulated to reflect interfacial energy anisotropy,<sup>[25]</sup> and  $B_{\alpha\beta}$  is an anisotropic elasticity matrix based on the Green function solution.<sup>[7]</sup> The term  $\tilde{\phi}_\alpha$  is the Fourier transform of  $\phi_\alpha$ , and the asterisk stands for complex conjugate. A necessary condition for a saddle point is given by a vanishing functional variation

$$\delta\Phi = 0 \quad [2]$$

where  $\Phi \equiv G - \lambda C$ ,  $C = C[\{\phi_\alpha\}]$  stands for additional physical constraints on the phase fields, and  $\lambda$  is the Lagrange multiplier. An example of the constraint is a mass conservation condition:  $C \equiv \int \phi(\mathbf{x}) d\mathbf{x} = \text{const}$ , where the phase field  $\phi$  is a concentration field. In this case,  $\lambda$  becomes the chemical potential of the reservoir, and  $\Phi$  becomes the grand potential.

To search for the solution to Eq. [2], the NEB method generates a chain of replicas (nodes) of microstructural configurations that approximately pass the saddle point. The “force” on node  $i$  ( $i = 0..N$ ,  $i = 0$  is the initial metastable energy minimum and the first NEB node,  $i = N$  is the last NEB node) is evaluated as<sup>[16]</sup>

$$\mathbf{F}_i = \mathbf{F}_i^s \parallel + \mathbf{F}_i^p \perp \quad [3]$$

It is a sum of a spring-type force  $\mathbf{F}_i^s$  determined by the relative distance between adjacent nodes and a potential force  $\mathbf{F}_i^p - \delta\Phi/\delta\phi_i$  ( $\phi_i$  represents the node  $i$  microstructural configuration, a  $MP$ -dimensional vector which is the numerically discretized version of  $\phi \equiv \{\phi_\alpha(\mathbf{x}) : \alpha = 1, \dots, P\}$ ) determined by the total energy surface. The subscripts  $\parallel$  and  $\perp$  stand, respectively, for the parallel and perpendicular component of the forces resolved on the local tangent of the node, which is evaluated from the energy ( $\Phi$ ) of the node and its immediate neighbors along the chain.<sup>[16]</sup> Each node, except for the two fixed ends, is relaxed iteratively subject to the force  $\mathbf{F}_i$ , which is simultaneously updated, until the chain converges to the MEP.

For problems of stress-driven nucleation and nucleation in phase transformations, the original NEB method was found to be inefficient, because the final minima could be very far from the saddle point and too many nodes were required to describe the downhill

portion of the MEP. A so-called “free-end” modification to the NEB method greatly improves the efficiency,<sup>[23,24]</sup> by allowing the last node  $N$  not to be a minimum, which furthermore moves to “swing” the band to improve its posture. The force on node  $N$  is

$$\mathbf{F}_N = \mathbf{F}_{N,N-1}^s - \frac{\mathbf{F}_{N,N-1}^s \cdot \mathbf{F}_N^p}{\mathbf{F}_N^p \cdot \mathbf{F}_N^p} \mathbf{F}_N^p \quad [4]$$

where  $\mathbf{F}_{N,N-1}^s$  is the spring force between node  $N-1$  and node  $N$ . It can be seen that when node  $N$  moves along  $\mathbf{F}_N$ , its energy is unchanged; thus, node  $N$  is constrained to move on an energy contour (isosurface) and would neither be “pulled up” on the band nor “drop down” to the minimum far away, thus maintaining the node density around the saddle point. In practice, there is a numerical truncation error in the dynamics, so we may also run a quasi-Newton step after Eq. [4]:

$$\Delta\phi_N = \frac{\kappa(\Phi_N - \Phi_N^{\text{desired}})}{\mathbf{F}_N^p \cdot \mathbf{F}_N^p} \mathbf{F}_N^p \quad [5]$$

where  $0 < \kappa \leq 1$ , and  $\Phi_N^{\text{desired}}$  is the desired potential. One can, for instance, set  $\Phi_N^{\text{desired}} = \Phi_0 - 0.1$  eV; *i.e.*, the free-end configuration is constrained to have  $-0.1$  eV lower energy than the initial metastable configuration, separated by the activation energy barrier. It can be proven that when the algorithm converges, node  $N$  will swing to be exactly sitting on the MEP.

### III. CRITICAL NUCLEUS IN CUBIC $\rightarrow$ TETRAGONAL TRANSFORMATION

With the NEB method, the critical nucleus can be accurately searched on a high-dimensional phase-field total free energy landscape that includes various crystal-line effects such as interfacial energy anisotropy, misfit elastic strain, *etc.*, as well as interactions with existing matrix defects (such as surfaces and grain boundaries, dislocations, inclusions, *etc.*). In what follows, a study of critical nucleus of a tetragonal phase in a cubic phase matrix is used to demonstrate the validity of this

approach. In particular, the effect of misfit strain level on the configuration and energy of critical nucleus is examined. We first provide a two-dimensional (2-D) analogue of the transformation to make a direct comparison to the nucleus generated by the Langevin dynamics. In both 2-D and three-dimensional cases, the chemical free energy is constructed as a 2-4-6 polynomial

$$f(\{\phi_\alpha\}) = \Delta f_0 \left[ \frac{A_1}{2} \sum_\alpha \phi_\alpha^2(\mathbf{x}) - \frac{A_2}{4} \sum_\alpha \phi_\alpha^4(\mathbf{x}) + \frac{A_3}{6} \left( \sum_\alpha \phi_\alpha^2(\mathbf{x}) \right)^3 \right] \quad [6]$$

with coefficients  $A_1 = 0.2$ ,  $A_2 = 12.8$ , and  $A_3 = 12.6$  that gives the cubic phase at  $\phi = 0$ , the tetragonal phase at  $\phi = \pm 1$ , and the energy difference between the cubic and tetragonal phases equal to  $\Delta f_0$  (Figure 1). The index  $\alpha$  labels the orientational variant. Note that the example considered here is a congruent transformation, and hence, only a nonconserved field is used. It may represent either a cubic  $\rightarrow$  tetragonal ordering or a cubic  $\rightarrow$  tetragonal martensitic transformation.

#### A. Critical Nucleus in Two Dimensions

In a 2-D analogue, the tetragonal precipitates form two orientation variants in the cubic phase matrix. Without considering dilatational components, one can formulate the stress-free transformation strains (SFTS) of the two variants as

$$\varepsilon_{ij}^T(1) = \varepsilon_0 \begin{pmatrix} 1 & 0 \\ 0 & -1 \end{pmatrix}, \quad \varepsilon_{ij}^T(2) = \varepsilon_0 \begin{pmatrix} -1 & 0 \\ 0 & 1 \end{pmatrix} \quad [7]$$

where  $\varepsilon_0$  is a constant. A relatively large ratio of elastic energy to chemical energy:  $\xi \equiv \mu\varepsilon_0^2/\Delta f_0 = 1$  ( $\mu$  is the shear modulus) is assumed. This results in a strong spatial correlation among the precipitating tetragonal domains in a partially developed microstructure, as shown in Figure 2(a). The simulation grid is  $256 \times 256$ . The grid size,  $l_0$ , characterizes the length unit and is

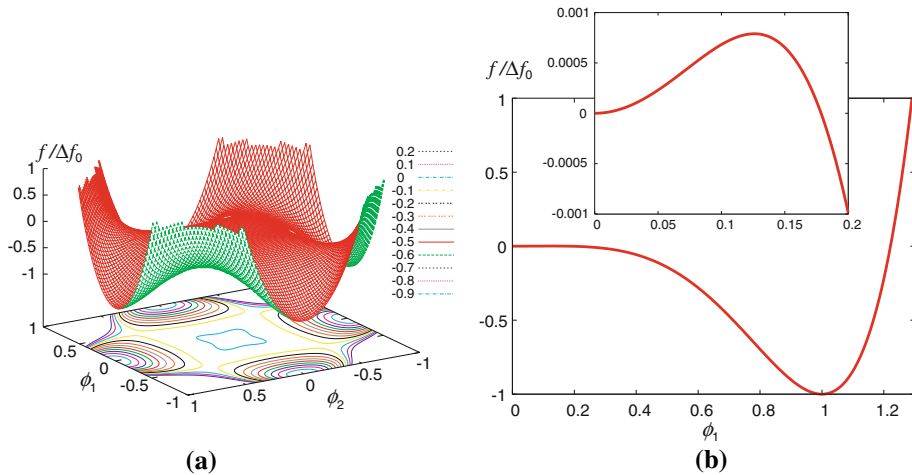


Fig. 1—The chemical free energy density plotted (a) in  $\phi_1 - \phi_2$  plane and (b) along  $\phi_1$  (with  $\phi_2 = 0$ ). A shallow metastable cubic phase is at  $\phi_1 = \phi_2 = 0$ . The tetragonal phase is at  $\phi_1 = 1$  or  $\phi_2 = 1$ .

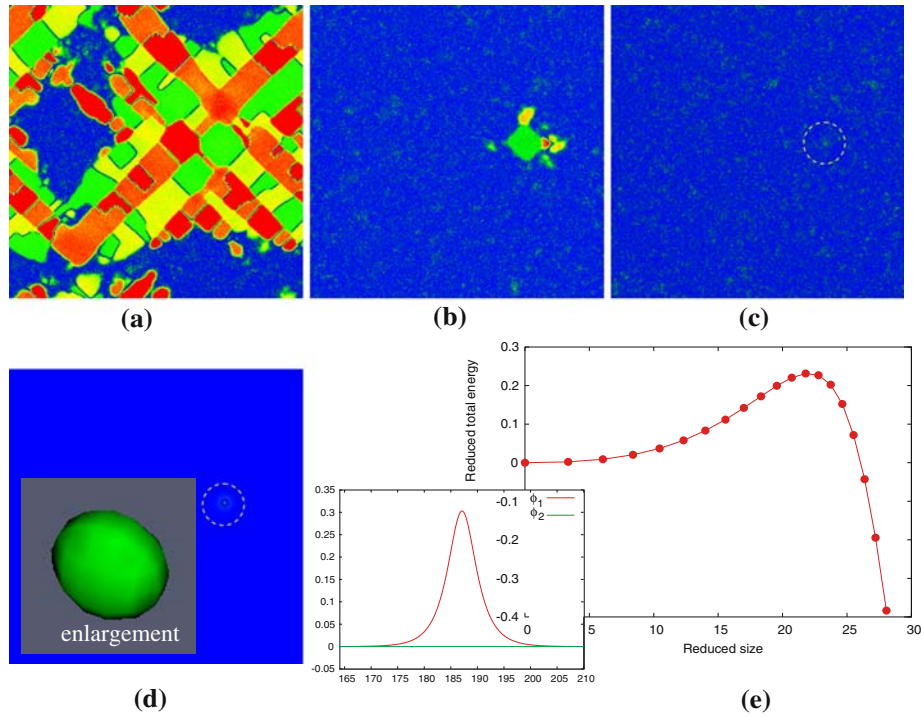


Fig. 2—(a) through (c) Microstructural evolution during a cubic  $\rightarrow$  tetragonal transformation in 2-D simulated by Langevin dynamics of phase field method. (b) A supercritical configuration at an earlier moment of (a). Use this as the end configuration in the NEB calculation gives (e) the nucleation barrier and the critical nucleus configuration (in the dashed circle in (d)), which is compared to a near-critical configuration (c) that is traced back from (b) in the Langevin dynamics. The energy is normalized by  $\Delta f_0 l_0^2$ , where  $l_0$  is the grid size.

determined by material parameters ( $\Delta f_0$  and interface energy  $\sigma$ ) when the model is applied to a particular system. The microstructure is obtained from an initially homogeneous cubic phase matrix with constantly applied thermal fluctuations *via* the Langevin force. Even with a very shallow potential energy well at the metastable cubic phase (Figure 1(b)), the nucleation free energy barrier is significant. An *artificially large* amplitude of the Langevin force fluctuations has to be applied in order to observe any nucleation event within a computationally affordable simulation time, similar to the first step in temperature-accelerated molecular dynamics simulations.<sup>[26]</sup>

In the FE-NEB calculations, one of the configurations (Figure 2(b)) generated by the conventional phase field dynamics with Langevin fluctuations is used as the initial chain-of-state end configuration. It is a supercritical configuration because it would continue to grow even if the Langevin force terms were turned off. The activation energy barrier then optimized with the FE-NEB method is given in Figure 2(e). The profiles shown in the inset indicate that the critical nucleus has a single-variant configuration, although the fully developed microstructure is a two-variant polytwinned microstructure. This indicates that the highly spatially correlated polytwinned domain structure is formed by strain-induced correlated nucleation and autocatalytic effect rather than by a collective process observed in the martensitic nucleation.<sup>[27]</sup> The order parameter in the nucleus is found to be considerably smaller than its equilibrium value for a bulk phase ( $\phi = 1$ ), which indicates nonclassical nucleation. Further relaxation of

the saddle-point configuration with the conventional phase-field dynamic equation did not show noticeable change (neither growth nor shrinkage) over a lengthy period of time, indicating we have indeed found a stationary point. For comparison, we examined the nucleus produced in the Langevin dynamics by tracing the configuration in Figure 2(b) back to the moment when it becomes barely stable (shown in Figure 2(c)). The configuration is found in qualitative resemblance to the critical nucleus identified by the NEB method (Figure 2(d)). However, the former should not be identified as a critical nucleus, and the corresponding energy is much higher than the actual activation energy barrier because of the artificially large Langevin fluctuations over the entire matrix.

### B. Critical Nucleus in Three Dimensions

Similar to the 2-D case, if we consider a pure shear transformation, the SFTSs of the three orientation variants of the tetragonal phase can be described by

$$\begin{aligned} \varepsilon_{ij}^T(1) &= \varepsilon_0 \begin{pmatrix} 2 & 0 & 0 \\ 0 & -1 & 0 \\ 0 & 0 & -1 \end{pmatrix}, & \varepsilon_{ij}^T(2) &= \varepsilon_0 \begin{pmatrix} -1 & 0 & 0 \\ 0 & 2 & 0 \\ 0 & 0 & -1 \end{pmatrix}, \\ \varepsilon_{ij}^T(3) &= \varepsilon_0 \begin{pmatrix} -1 & 0 & 0 \\ 0 & -1 & 0 \\ 0 & 0 & 2 \end{pmatrix} \end{aligned} \quad [8]$$

Figure 3(a) shows a polytwin structure consisting of alternating layers of two tetragonal variants. The



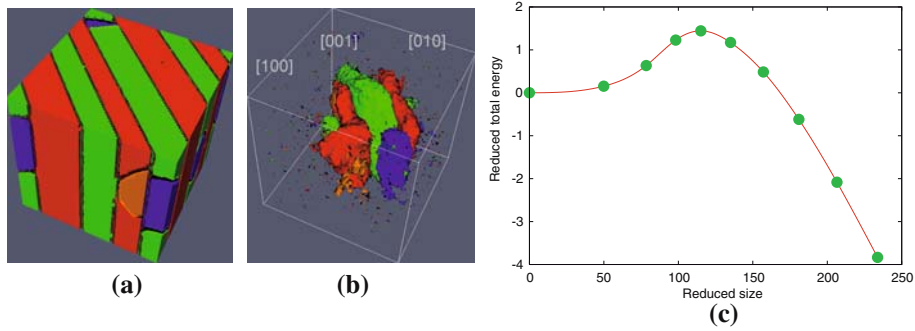


Fig. 3—(a) A polytwin structure consisting of two orientational variants of the tetragonal phase generated by phase-field dynamics with Langevin fluctuations. (b) The microstructure at an earlier moment used as the FE configuration in the NEB calculation for the MEP shown in (c). The energy is normalized by  $\Delta f_0 l_0^3$ , where  $l_0$  is the grid size.

simulation is performed in a  $64 \times 64 \times 64$  cubic cell. In some layers, two domains (represented by different colors or different shades of gray within the same layer) in antiphase relation (corresponding to plus and minus sign in  $\phi$ ) are observed. The microstructure is produced by Langevin fluctuations applied constantly to an initially homogeneous cubic phase with  $\xi \equiv \mu v_0^2 / \Delta f_0 = 0.5$ . The establishment of the first stable fluctuation (nucleus) takes much longer time than the subsequent growth. As in the 2-D case, a partially transformed configuration (Figure 3(b)) is taken as the free end of NEB, while the other end node of NEB is fixed at the homogeneous cubic phase. The nucleation barrier is shown in Figure 3(c). The critical nucleus is found to be a single-variant particle. A close examina-

tion shows that it has an ellipsoidal shape with the “broad” face normal parallel to  $\langle 100 \rangle$  directions owing to the elastic energy. The sequence of configurations along the down-hill side of the MEP is shown in Figure 4. Along the MEP, the single-variant nucleus grows while maintaining its ellipsoidal shape (Figure 4(b)), until a second variant is formed spontaneously (Figure 4(c)) with the interface normal rotating simultaneously to  $\langle 110 \rangle$  twin boundary orientation. The subsequent growth takes a much faster pace *via* strain-induced formation of alternate tetragonal variants.

As the ratio of elastic energy to chemical energy increases the critical nucleus changes from a single-variant ellipsoid ( $\xi = 0.5$ ) to a two-variant twinned

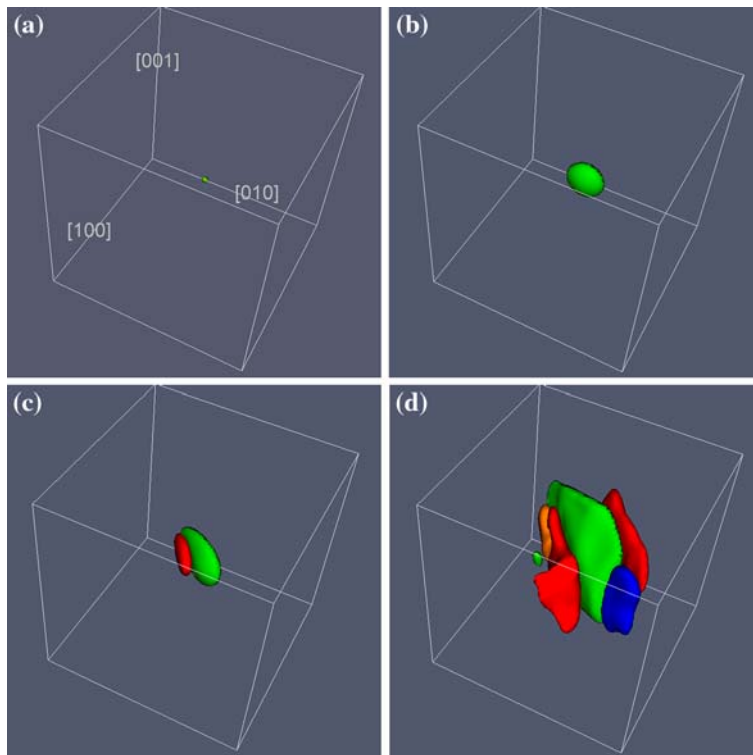


Fig. 4—(a) through (d) Configuration sequence of a tetragonal precipitate along the MEP showing emerging of the second variant and simultaneous rotation of the interface. (a) Critical nucleus consisting of a single variant.

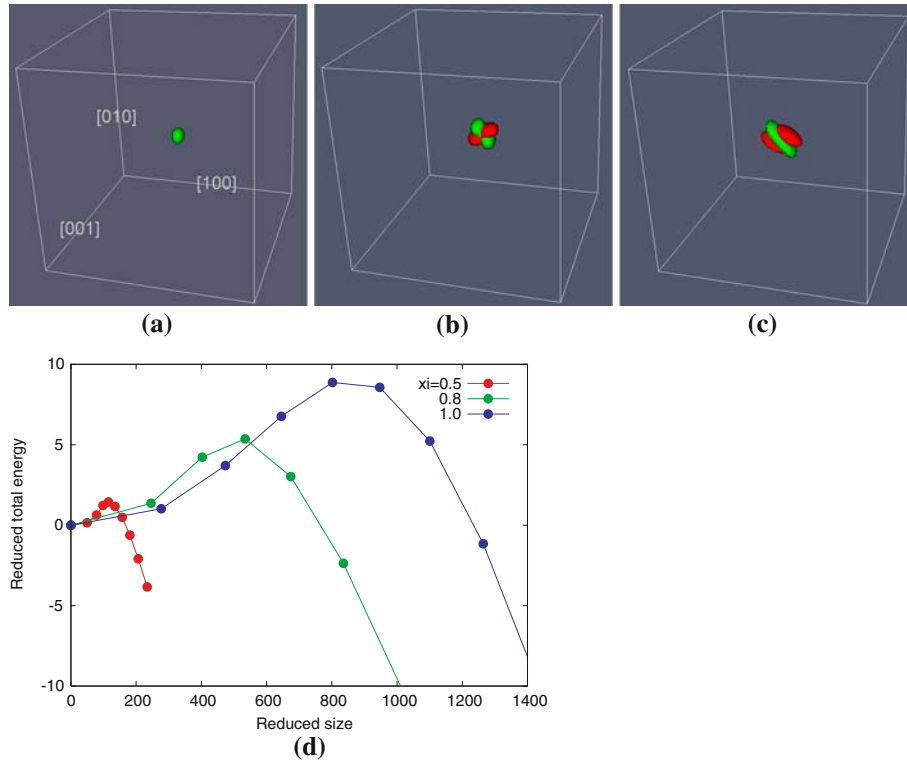


Fig. 5—Transition of morphology of the critical nucleus from a single variant to a two-variant configuration with increasing lattice misfit: (a)  $\xi = 0.5$ , (b) 0.8, and (c) 1.0. The corresponding nucleation barriers are shown in (d). Here, (a) is the same as Fig. 4(a) but from a different view angle.

structure ( $\xi = 1.0$ ), while an intermediate two-variant configuration is obtained at  $\xi = 0.8$  (Figure 5(a) through (c)). Since the chemical driving force is fixed in all these cases, this effect is solely determined by the competition between the interfacial energy and the elastic energy of the nucleus: at a relatively small elastic energy contribution, the interfacial energy minimization dominates the nucleation process. Nevertheless, the elastic energy still plays a role in producing the ellipsoidal shape of the nucleus. As the elastic energy contribution becomes larger, reduction in elastic energy by adopting an internally twinned two-variant configuration finally exceeds the increase in interfacial energy associated with the formation of the twin boundaries. Obviously, martensitic transformations belong to the latter category. It is seen in Figure 5(d) that the nucleation barrier and the size of the critical nucleus increase with increasing elastic energy contribution.

#### IV. DISCUSSION

Nucleation in solids is often complicated by crystal lattice mismatch between the parent and product phases, the anisotropies of nucleus-matrix interfaces and elastic moduli, and the presence of other lattice defects that carry either short-range or long-range interactions with the nucleus.<sup>[28–31]</sup> These complications have been treated rather routinely in the past by the phase field approach where nucleation has been treated by the use of

Langevin force terms in the stochastic phase field equations.<sup>[27,32–35]</sup> In principle, such a stochastic dynamic approach can perform statistical sampling of the entire configurational space and hence allows for quantitative description of the nucleation process. Since the long-range elastic, electrostatic, and magnetostatic interactions are included in the total phase field free energy functional, their effects on nucleation are included automatically. However, the Langevin force approach was found extremely inefficient in searching for saddle configurations.<sup>[36]</sup> Additionally, if one attempts to describe nucleation solely by the Langevin force approach in a quantitative manner, both length and time scales are limited by the microscopic degrees of freedom.<sup>[37]</sup> Currently, the use of the Langevin approach to nucleation in phase field simulations of microstructural evolution is qualitative in nature, and its applications are limited to site-saturation conditions.<sup>[27,32,33,35]</sup> As an alternative, an explicit nucleation algorithm was developed, which stochastically seeds nuclei in an evolving microstructure according to the nucleation rates evaluated as a function of local concentration, structure, and temperature<sup>[38]</sup> following the classical nucleation theory (in principle, the nonclassical nucleation theory as well). The coherency strain energy associated with the formation of a nucleus in an arbitrary pre-existing coherent microstructure in elastically anisotropic media can be incorporated into the activation energy of nucleation in the explicit algorithm.<sup>[39,40]</sup> This provides an efficient approach to

modeling coherent nucleation in an evolving mesoscale microstructure with quantitative agreement with the Langevin force approach. However, this approach requires the activation energy and critical nucleus configuration as essential input rather than output.

The activation energy of nucleation and critical nucleus configuration are essential kinetics properties of many solid-state processes including first-order phase transformations, formation of voids, cracks, and stacking faults, ferroelectric and ferromagnetic domains, *etc.* To find the critical nucleus and the activation energy, we have developed a new approach within the framework of the nonclassical nucleation theory and the phase field method. Instead of using exclusively the phase field method to drive Langevin fluctuation-dissipation kinetics, we combined the energetic part of the phase field method with the NEB method to find the critical nucleus and the associated MEP. Using the conventional Langevin approach to nucleation in phase field simulations to generate end configurations and the newly developed FE-NEB technique, we show that this approach can be used as an efficient and reliable tool to study nucleation in solids. Since the only inputs required by the NEB calculation are the total energy functional and its first variational derivatives, the physical nature of nucleation is solely dependent on the phase field energetics. This approach can be extended to any thermally activated processes that can be modeled by phase field energetics, including nucleation of stacking faults and dislocation loops, voids and microcracks, and ferroelectric and ferromagnetic domains. The consideration of heterogeneous nucleation at pre-existing crystalline defects in the model is straightforward. An example of such is the study of dislocation shearing of  $\gamma'$  precipitates in Ni-base alloys, where superlattice stacking faults are formed either homogeneously or heterogeneously in the  $\gamma'$  particles under external load through an activation process.<sup>[17]</sup>

Physically, the end configurations generated by the Langevin fluctuations represent the precipitate configurations that are approximately on a MEP and thus are the energetically more probable ones in the transformation. The fluctuation-dissipation process provides a statistical sampling in the configurational space that often yields a physically more reasonable configuration than one designed by hands. With the FE-NEB, the end configurations are not required to be strictly on the MEP—deviations due to dynamic effects may be relaxed by the treatment on the free end. Furthermore, in a complex transformation, where multiple low-energy configurations exist, multiple Langevin sampling may be performed, each to map out an MEP in a global energy landscape. The true saddle point for nucleation is then identified from the lowest one among them. By this means, the artifact in the design of the NEB end configuration may be eliminated.

For the cubic  $\rightarrow$  tetragonal transformations considered in the current study, the ratio of the elastic energy to the chemical free energy is shown to play an important role in determining both the morphology and the energy of a critical nucleus. Relatively large elastic energy contribution results in a collective nucle-

ation that produces directly a twin-related multivariant nucleus, while relatively small elastic energy contribution results in a sequential nucleation where the critical nucleus is a single-variant particle and the polytwinned structure develops at later stages through stress-induced autocatalytic events. This is because when the elastic energy contribution is dominant, coupling of two variants reduces the per-volume elastic energy even at a cost of extra twin boundary energy, and is more beneficial to the overall nucleation energy as compared to the formation energy of a single variant configuration. When the elastic energy contribution is relatively small, it is energetically more favorable to form a single-variant nucleus without generating the twin boundaries. When the particle grows bigger, the elastic energy gradually becomes dominant over the twin boundary energy and the particle adopts a polytwinned structure. An interesting nontrivial critical nucleus configuration (Figure 5(b)) has been identified at an intermediate value of the elastic energy to chemical free energy ratio.

## V. SUMMARY

To take advantage of the generality of the phase field total free energy functional that is formulated based on gradient thermodynamics and microelasticity theory, a new approach is developed for finding critical nucleus configuration and calculating activation energy in solid-state processes with least constraints on the transformation pathway. With the traditional Langevin force approach in the phase field method providing initial end configurations, a modified FE-NEB method is used to efficiently explore the phase field total free energy landscape and to locate the saddle points. For the cubic  $\rightarrow$  tetragonal transformation considered, even though the final microstructures are all multilayer polytwins, the critical nucleus configuration and activation energy are found to be strong functions of the ratio of elastic energy to chemical free energy. This new approach provides an efficient and completely general way to investigate the effect of various crystalline defects and external fields on nucleation in many solid-state processes.

## ACKNOWLEDGMENTS

We acknowledge support by the AFOSR MEANSII (Grant No. FA9550-05-1-0135) and ONR D3D (Grant No. N00014-05-1-0504) programs and the Ohio Supercomputer Center. The work of JL is also supported by Grant No. NSF DMR-0502711.

## REFERENCES

1. J.W. Cahn and J.E. Hilliard: *J. Chem. Phys.*, 1959, vol. 31, pp. 688–99.
2. J.W. Cahn and J.E. Hilliard: *J. Chem. Phys.*, 1958, vol. 28, pp. 258–67.
3. J.B. Rundle and W. Klein: *Phys. Rev. Lett.*, 1989, vol. 63, pp. 171–74.

4. J.R. Rice and G.E. Beltz: *J. Mech. Phys. Solids*, 1994, vol. 42, pp. 333–60.
5. R. Poduri and L.Q. Chen: *Acta Mater.*, 1996, vol. 44, pp. 4253–59.
6. A.C.E. Reid, G.B. Olson, and B. Moran: *Phase Transitions*, 1999, vol. 69, pp. 309–28.
7. A.G. Khachaturyan: *Theory of Structural Transformations in Solids*, John Wiley & Sons, New York, NY, 1983, pp. 198–212.
8. J.R. Rice: *J. Mech. Phys. Solids*, 1992, vol. 40, pp. 239–71.
9. Y. Wang, L.Q. Chen, and A.G. Khachaturyan: in *Computer Simulation in Materials Science—Nano/Meso/Macroscopic Space and Time Scales*, H.O. Kirchner, K.P. Kubin, and V. Pontikis, eds., Kluwer Academic Publishers, Dordrecht/Boston/London, 1996, pp. 325–71.
10. Y. Wang and L.Q. Chen: *Methods in Material Research*, John Wiley & Sons, Inc. New York, NY, 2000, pp. 2a.3.1–2a.3.23.
11. A. Karma: in *Encyclopedia of Materials: Science and Technology*, K.H.J. Buschow, R.W. Cahn, M.C. Flemings, B. Ilshner, E.J. Kramer, and S. Mahajan, eds., Elsevier, Oxford, United Kingdom, 2001, vol. 7, pp. 6873–86.
12. L.Q. Chen: *Ann. Rev. Mater. Res.*, 2002, vol. 32, pp. 113–40.
13. Y.U. Wang, Y.M. Jin, and A.G. Khachaturyan: in *Handbook of Materials Modeling, Part B: Models*, S. Yip, ed., Springer, New York, NY, 2005, pp. 2287–305.
14. Y.A. Chu, B. Moran, and G.B. Olson: *Metall. Mater. Trans. A*, 2000, vol. 31A, pp. 1321–31.
15. L. Gránásy, T. Börzsönyi, and T. Pusztai: *Phys. Rev. Lett.*, 2003, vol. 88, pp. 206105-1–4.
16. G. Henkelman and H. Jonsson: *J. Chem. Phys.*, 2000, vol. 113, pp. 9978–85.
17. C. Shen, J. Li, M.J. Mills, and Y. Wang: in *Integral Materials Modeling*, G. Gottstein, ed., Wiley-VCH, Heidelberg, 2007, pp. 243–52.
18. E. Wigner: *Trans. Faraday Soc.*, 1938, vol. 34, pp. 29–41.
19. H. Jonsson, G. Mills, and K.W. Jacobsen: in *Classical and Quantum Dynamics in Condensed Phase Simulations*, B.J. Berne, G. Ciccotti, and D.F. Coker, eds., World Scientific, NJ, 1998, pp. 385–404.
20. G. Mills and H. Jonsson: *Phys. Rev. Lett.*, 1994, vol. 72, pp. 1124–27.
21. G. Mills, H. Jonsson, and G.K. Schenter: *Surf. Sci.*, 1995, vol. 324, pp. 305–37.
22. G. Henkelman, B.P. Uberuaga, and H. Jonsson: *J. Chem. Phys.*, 2000, vol. 113, pp. 9901–04.
23. T. Zhu, J. Li, A. Samanta, H.G. Kim, and S. Suresh: *Proc. Nat. Acad. Sci. USA*, 2007, vol. 104, pp. 3031–36.
24. J. Li, P.A. Gordon, and T. Zhu: unpublished research, 2007.
25. G.B. McFadden, A.A. Wheeler, R.J. Braun, S.R. Coriell, and R.F. Sekerka: *Phys. Rev. E*, 1993, vol. 48, pp. 2016–24.
26. M.R. Sorensen and A.F. Voter: *J. Chem. Phys.*, 2000, vol. 112, pp. 9599–606.
27. Y. Wang and A.G. Khachaturyan: *Acta Metall. Mater.*, 1997, vol. 45, pp. 759–73.
28. K.C. Russell: in *Phase Transformations*, H.I. Aaronson, ed., ASM, Metals Park, OH, 1970, pp. 219–68.
29. H.I. Aaronson and J.K. Lee: in *Lectures on the Theory of Phase Transformations*, H.I. Aaronson, ed., TMS, Warrendale, PA, 1999, pp. 165–229.
30. J. Li: *MRS Bull.*, 2007, vol. 32, pp. 151–59.
31. S.N. Luo, L.Q. Zheng, A. Strachan, and D.C. Swift: *J. Chem. Phys.*, 2007, vol. 126, pp. 034505-1–7.
32. Y. Wang, L.Q. Chen, and A.G. Khachaturyan: in *Solid-Solid Phase Transformations*, W.C. Johnson, J.M. Howe, D.E. Laughlin, and W.A. Soffa, eds., TMS, Warrendale, PA, 1994, pp. 245–65.
33. Y. Wang, H.Y. Wang, L.Q. Chen, and A.G. Khachaturyan: *J. Am. Ceram. Soc.*, 1995, vol. 78, pp. 657–61.
34. Y. Le Bouar, A. Loiseau, and A.G. Khachaturyan: *Acta Mater.*, 1998, vol. 46, pp. 2777–88.
35. Y.H. Wen, Y. Wang, and L.Q. Chen: *Philos. Mag. A*, 2000, vol. 80, pp. 1967–82.
36. H.Y. Wang, Y.Z. Wang, T. Tsakalakos, S. Semenovskaya, and A.G. Khachaturyan: *Philos. Mag. A*, 1996, vol. 74, pp. 1407–20.
37. K. Binder: *Rep. Progr. Phys.*, 1987, vol. 50, pp. 783–859.
38. J.P. Simmons, C. Shen, and Y. Wang: *Scripta Mater.*, 2000, vol. 43, pp. 935–42.
39. C. Shen, J.P. Simmons, and Y. Wang: *Acta Mater*, 2006, vol. 54, pp. 5617–30.
40. C. Shen, J.P. Simmons, and Y. Wang: *Acta Mater*, 2007, vol. 55, pp. 1457–66.